

Measurement of triple differential photon plus jet cross section by DØ

Ashish Kumar (*for the DØ collaboration*)

Department of Physics, The State University of New York at Buffalo, NY 14260, USA.

E-mail: ashishk@fnal.gov

Abstract. We report on a new measurement of triple differential cross section for the process $p\bar{p} \rightarrow \gamma + jet + X$ in $p\bar{p}$ collisions at $\sqrt{s}=1.96$ TeV by the DØ Collaboration at Fermilab based on dataset corresponding to an integrated luminosity of 1.1 fb^{-1} .

1. Introduction

The photon plus jet (“ $\gamma + jet$ ”) events have the sheer advantage that the isolated photons are mostly “direct” photons, which emerge unaltered from the hard-scattering and provide clean probe of the parton level dynamics [1]. Together with the jet kinematics, these events shed more light on the underlying QCD dynamics. The parton level subprocesses include the Compton-scattering $gq \rightarrow q\gamma$ which dominates in a wide kinematic range and the annihilation subprocess $q\bar{q} \rightarrow g\gamma$. Studies of “ $\gamma + jet$ ” events, therefore, offer precision tests of perturbative QCD as well as information on the gluon density inside the colliding hadrons. Photons from hadron (π^0, η , etc.) decays and the bremsstrahlung process provide the major background particularly at low transverse momentum (p_T). However, their contribution is suppressed after application of tight photon isolation criteria.

Using about 1.1 fb^{-1} of Tevatron Run II data, DØ has measured the triple differential cross section for $p\bar{p} \rightarrow \gamma + jet + X$ process with a photon in the central pseudorapidity region, $|\eta^\gamma| < 1.0$, and a leading jet with $p_T > 15$ GeV in either the central ($|\eta^{jet}| < 0.8$) or the forward ($1.5 < |\eta^{jet}| < 2.5$) region. The photon p_T (p_T^γ) varies from 30 to 300 (200) GeV for the central (forward) jets. The analysis considers four kinematic regions differing in $|\eta^\gamma|$ and $|\eta^{jet}|$: (1) both central and same side, (2) both central and opposite side, (3) central photon, forward jet and same side, and (3) central photon, forward jet and opposite side. The kinematic region in the $x - Q^2$ plane covered by the analysis (approximately $0.007 \leq x \leq 0.7$ and $0.9 \times 10^3 \leq Q^2 \leq 0.4 - 0.8 \times 10^5 \text{ GeV}^2$) significantly extends previous measurements.

2. Event Selection and Background Suppression

Photons are identified in the DØ detector as isolated energy deposits in the electromagnetic (EM) calorimeter consisting of 4 layers, EM1-EM4. Photon candidates are reconstructed with a cone algorithm with cone size $\mathcal{R} = \sqrt{(\Delta\eta)^2 + (\Delta\phi)^2} = 0.2$. Candidates are selected if there is significant energy in the EM layers ($> 96\%$), and the probability to have a matched track is less

than 0.1%, and they satisfy an isolation requirement $[E_{total}(0.4) - E_{EM}(0.2)]/E_{EM}(0.2) < 0.07$, where $E_{total}(0.4)$ and $E_{EM}(0.2)$ are the total and EM energies within cone size of 0.4 and 0.2, respectively. We also limit the energy weighted cluster width in the finely-segmented EM3 layer. Potential backgrounds from W boson decays to electrons and cosmes were suppressed by the cut on missing transverse energy $E_T^{miss} < 12.5 + 0.36 p_T^\gamma$. Three discriminating variables were used for further background suppression: the number of EM1 cells with energy > 0.4 GeV within $\mathcal{R} < 0.2$, the fraction of the EM cluster energy deposited in the EM1 layer, and the scalar sum of track p_T in the ring of $0.05 \leq \mathcal{R} \leq 0.4$ (with $p_T^{track} > 0.4$ GeV) around the photon cluster direction. These variables turned out to be very efficient for background suppression and show consistent behavior for MC/data electrons from $Z \rightarrow ee$ events. They are used as an input to an artificial neural network (NN) optimized for pattern recognition. An additional cut on the NN output $O_{NN} > 0.7$ is applied. The total photon selection efficiency is about 62% at $p_T^\gamma \simeq 30$ GeV and increases to a plateau of $\geq 70\%$ at $p_T^\gamma \geq 70$ GeV. The event is required to have at least one hadronic jet reconstructed with a cone algorithm of $\mathcal{R} = 0.7$. The photon candidate and the most energetic jet were required to be well separated, $d\mathcal{R}(\gamma, jet) > 0.7$. The total number of “ $\gamma + jet$ ” events remaining in Regions 1–4 after application of all the selection criteria is about 2.4 million ($\sim 34.4\%$, 30.2% , 20.1% , 13.3% in Regions 1 to 4). These events are used to calculate the cross sections in 15 p_T^γ bins varied from 30 to 300 GeV for Regions 1, 2 and in 13 p_T^γ bins varied from 30 to 200 GeV for Regions 3, 4.

The selected signal sample still contains a sizeable background dominated by the di-jet events when one jet fluctuates to a well isolated EM cluster. These jets are primarily composed of one or more neutral mesons that decay into photons, and may also be accompanied by other soft hadrons whose energies are deposited in the EM portion of the calorimeter. Since the signal events cannot be identified on an event-by-event basis, their fraction is determined statistically for a given p_T^γ bin. The photon purity (\mathcal{P}) is determined by fitting the ANN distribution in data to a linear combination of the predicted ANN distributions for the signal and the background.

3. Calculation of “ $\gamma + jet$ ” Cross Section and Comparison with Theory

The triple differential “ $\gamma + jet$ ” cross section is obtained using the relation:

$$\frac{d^3\sigma}{dp_T^\gamma d\eta^\gamma d\eta^{jet}} = \frac{N \mathcal{P} U}{L_{int} \Delta p_T^\gamma \Delta \eta^\gamma \Delta \eta^{jet} \epsilon_s^{\gamma+jet}} \quad (1)$$

where N is the number of “ $\gamma + jet$ ” candidates in the selected sample, L_{int} is the integrated luminosity, $\epsilon_s^{\gamma+jet}$ is the signal selection efficiency, Δp_T^γ , $\Delta \eta^\gamma$ and $\Delta \eta^{jet}$ are the bin sizes in p_T^γ , η^γ and η^{jet} . The factor U corrects the cross section for the finite resolution of the calorimeter. The measured cross sections are shown in Fig. 1 as a function of p_T^γ with the full experimental (systematic \oplus statistical) errors. The largest uncertainties are caused by the purity estimation, photon and jet selections and luminosity. Statistical errors vary from 0.1% in the first p_T^γ bin to 13 – 20% in the last bin while systematic errors are within 10 – 15% depending on region. The superimposed theoretical curve corresponds to the next-to-leading order (NLO) QCD predictions based on the JETPHOX program [2] with the CTEQ6.1M set of parton distribution functions (PDF’s) and BFG set of fragmentation functions [6]. The choice of renormalization (μ_R), factorization (μ_F) and fragmentation (μ_f) scales used is $\mu_R = \mu_F = \mu_f = p_T^\gamma f(y^*)$ with $f(y^*) = ([1 + \exp(-2|y^*)|]/2)^{1/2}$ and $y^* = 0.5(\eta^\gamma - \eta^{jet})$.

The ratios of the measured cross sections to the NLO predictions are presented in Fig. 1 for the regions 1 and 3. The shape of data/theory in regions 2 and 4 is similar to that observed in regions 1 and 3, respectively. Only the statistical uncertainties are shown in the data points. The p_T dependent systematic uncertainties are shown on the plots separately by a shaded region. The scale dependence of the predictions is estimated by varying the scales by factors of two which

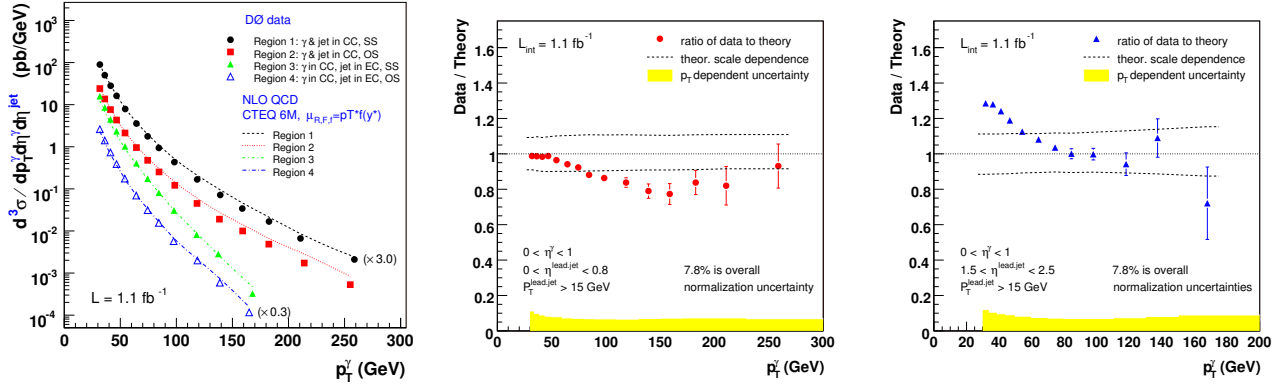


Figure 1. Left: The p_T^γ spectrum of measured “ $\gamma + jet$ ” cross sections for the four Regions along with the NLO predictions by JETPHOX [2] shown as curves (they are scaled by factors 3.0 & 0.3 for Regions 1 & 4, respectively). The data are plotted at the p_T^γ -weighted average of the fit function for each bin. Middle: The ratio of the measured to the predicted cross section in *Region 1*. Dashed lines represent the effect of scale variations by factor of two. Right: similar ratio but for *Region 3*. Refer to the text for the details.

yield uncertainties of 9–11% for Regions 1–3 and 18–20% for Region 4. The choice of different parameterizations of PDF’s lead to variations in the data/theory ratios up to about 10% for Regions 1–3 and up to $\sim 20\%$ for Region 4. The results of the measurements show a significant deviation from the NLO predictions for $p_T^\gamma > 100$ GeV for the regions 1 and 2 and for $p_T^\gamma < 50$ GeV for the Region 3. Such pattern of deviations in the data-to-theory ratios have earlier been encountered by the UA2 [3], CDF [4] and DØ [5] analyses. These results do indicate the need of a better theoretical understanding of the processes with production of high energetic photons. In particular, calculations enhanced for soft-gluon contributions are expected to provide a better description of the data at low p_T^γ in Region 3.

In order to reduce the systematic uncertainties, we have also calculated ratios of the measured cross sections between different regions. Most systematic uncertainties related to object (γ & jet) identification and luminosity are canceled in the ratios. The only systematic uncertainties that survive are related to the “ $\gamma + jet$ ” event purities (since they differ a little between the four regions) and the jet selection efficiency when we calculate ratios with the central jet in one region and the forward jet in another region. The overall experimental uncertainty estimated in such a way is about 3.5–9% for $44 < p_T^\gamma < 110$ GeV and becomes larger for smaller p_T^γ (due to systematics) and larger p_T^γ (due to statistics). Also, the scale uncertainty in the ratios is noticeably reduced; to the level of just 1–3% for Regions 1–3 and up to 3–8% for Region 4. In general, the shapes of the measured cross section ratios in data are qualitatively reproduced by the theory but we observe a quantitative disagreement for some kinematic regions even after taking into account the overall (experimental and theoretical scale) uncertainty. It is especially noticeable for the cross section ratios between Regions 1 & 3 as well as between Regions 2 & 3.

References

- [1] Owens J F 1987 *Rev. Mod. Phys.* **59** 465.
- [2] Catani S, Fontannaz F, Guillet J P and Pilon E 2002 *JHEP* **05** 028.
- [3] Alitti J *et al* (UA2 Collaboration) 1991 *Phys. Lett. B* **263** 544.
- [4] Acosta D *et al* (CDF Collaboration) 2002 *Phys. Rev. D* **65** 112003.
- [5] Abazov V *et al* (DØ Collaboration) 2006 *Phys. Lett. B* **639**, 151.
- [6] Bourhis L, Fontannaz M and Guillet J P 1998 *Eur. Phys. J. C* **2** 529.